Journal of the Ceramic Society of Japan 118 [8] 669-673 2010 Paper

Effect of bottom electrode structure on electrical properties of $BaTiO_3$ thin films fabricated by CSD method

Naonori SAKAMOTO,† Haruna YOSHIOKA, Junpei SUZUKI,* Toshimasa SUZUKI,* Naoki WAKIYA and Hisao SUZUKI**

Department of Materials Science and Chemical Engineering, Shizuoka University, 3–5–1 Johoku, naka-ku, Hamamatsu, Shizuoka 432–8561
***Taiyo Yuden Co Ltd, R&D Center, 5607–2 Nakamuroda-machi, Takasaki, Gunma 370–3347**
****Graduate School of Science and Technology, Shizuoka University, 3–5–1 Johoku, naka-ku, Hamamatsu, Shizuoka 432–8561**

$BaTiO_3$ (BT) based perovskite films are expected as ferroelectric and piezoelectric materials alternating $Pb(Zr,Ti)O_3$ (PZT) films which involve toxicity of the lead. In the present study, we focus effects of bottom electrode structures on electrical properties of the BT films fabricated by Chemical Solution Deposition (CSD) method. The BT films were fabricated on 1–6 layered $LaNiO_3$ (LNO) bottom electrode on Si or $Pt/Ti/SiO_2/Si$ substrate. The dielectric constant of the BT films fabricated on $LNO/Pt/Ti/SiO_2/Si$ substrate showed higher values than that on the LNO/Si substrate. The dielectric constant and piezoelectric properties increased with increasing layer numbers of the LNO. The microstructure and crystal structure of the BT films was studied by means of X-ray diffraction, scanning electron microscopy (SEM), and scanning transmission electron microscopy (STEM).

Key-words : $BaTiO_3$, $LaNiO_3$, Thin film, Ferroelectric, Bottom electrode

[Received May 24, 2010; Accepted July 15, 2010]

1. Introduction

Thin films of dielectrics/ferroelectrics with perovskite structure are of great interest for a variety of integrated devices, e.g. dynamic random access memory (DRAM), decoupling capacitors, multi-layered ceramic capacitors (MLCC), pyroelectric infrared (IR) sensors, and piezoelectric microactuators.[1)–15)] When focused on ferroelectric and piezoelectric properties, lead oxide-based ferroelectrics, represented by lead zirconate titanate, $Pb(Zr,Ti)O_3$ (PZT), are the most popular one due to their excellent ferroelectric and piezoelectric properties. However, because of the toxicity of the lead oxide, alternative lead-free ferroelectric/piezoelectric film is desired. Recently, lead-free piezoelectric films are being extensively investigated to replace PZT based films. $BaTiO_3$ (BT) is one of the main lead-free electronics for dielectric, piezoelectric, and electro-optic applications.[16)–26)] In order to obtain highly oriented BT film, many researches try to grow them on buffer layers; highly oriented PZT films can be deposited on Pt coated Si substrate using LNO, TiO_2, or PbO as buffer.[27)–31)] As Guo et al. reported,[23)] bottom layer of the film affects properties of the films electrically and morphologically. They reported electrical dielectric and piezoelectric properties of $BaTiO_3$ thin film on a $Pt/TiO_x/SiO_2/Si$ substrate using LNO buffer layer, where the LNO buffer layer on the surface of a Pt electrode is effective in enhancing the crystallinity of BT films and (100)-oriented BT films can be grown on the LNO buffer layer. Electrical properties of dielectric films fabricated on a substrate are influenced not only by the processing conditions, but also by several structural factors such as electrode materials and insertion of interlayer.[32),33)] In a practical sense, origins of these factors are interaction between the film and the electrode and are complicated because each factor contributes simultaneously to the film properties. In the present study, therefore, we demonstrate fabrication of BT films on Si substrate and $Pt/Ti/SiO_2/Si$ substrate with identical bottom electrode LNO with varying thickness in order to investigate effects of bottom electrode structures.

Among many kinds of film fabrication technique, chemical solution deposition (CSD) method is a candidate as a low cost process.[17)–19),23),34)] The CSD method basically requires conventional spin-coating system and furnaces for film preparation, therefore it does not require sophisticated vacuum system etc. Another advantage of the CSD method is a large area deposition with high homogeneity of the film on the substrate. These advantages are extremely important in the industrial meaning. Therefore in the present study, we report our investigation on the film fabricated by the CSD method.

2. Experimental

BT films and LNO electrodes were fabricated by CSD method. Preparation of the precursor solution for the dielectric films and electrodes were schematically shown in **Fig. 1**(a) and (b), respectively. 0.3 M LNO precursor solution was prepared by mixing $La(NO_3)_3{\cdot}6H_2O$ (lanthanum nitrate hexahydrate, Kanto Chemical Co. Inc., 99.99%), $(CH_3COO)_2Ni{\cdot}4H_2O$ (nickel acetate tetrahydrate, Kanto Chemical Co. Inc., 98.0%), and CH_3CH_2OH (absolute ethanol, Kanto Chemical Co. Inc., 99.0%) in a conical flask and subsequently stirring it for 3 h at 60°C. 0.1 M BT precursor solution was prepared from precursor solutions of Ba and Ti sources. The Ba solution was prepared by dissolving Ba metal (Nakarai tesque Inc., 99.0%) in $CH_4OC_2H_4OH$ (2-methoxyetanol, Kanto Chemical Co. Inc., 99.0%). The solution for the Ti was prepared by mixing $[(CH_3)_2CHO]_4Ti$ (titanium tetra-isopropoxide, Kanto Chemical Co. Inc., 97.0%) and the $CH_4OC_2H_4OH$ (2-methoxyetanol, Kanto Chemical Co. Inc.,

† Corresponding author: N. Sakamoto; E-mail: tnsakam@ipc.shizuoka.ac.jp

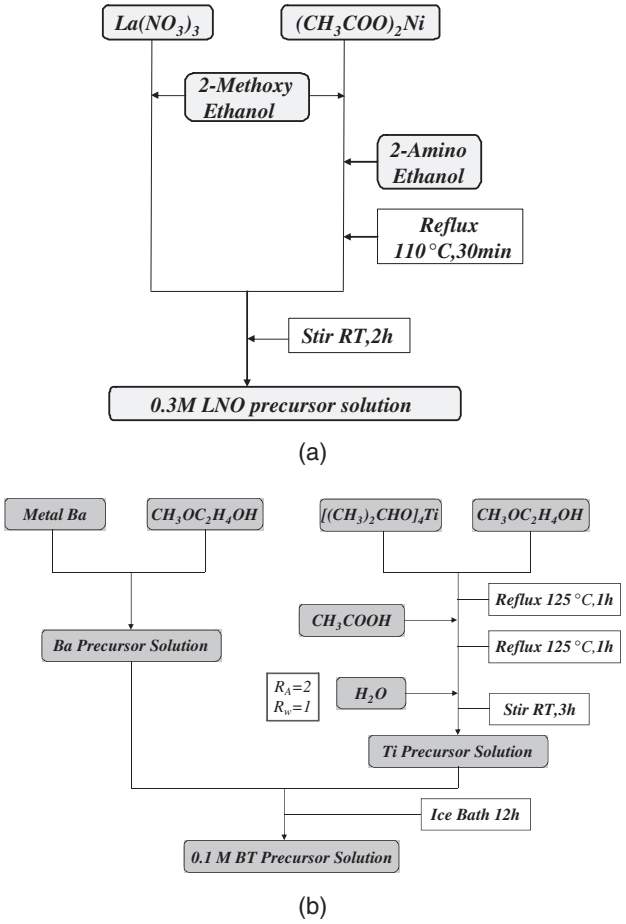

Fig. 1. Preparation of precursors for LNO electrode (a) and BT film (b).

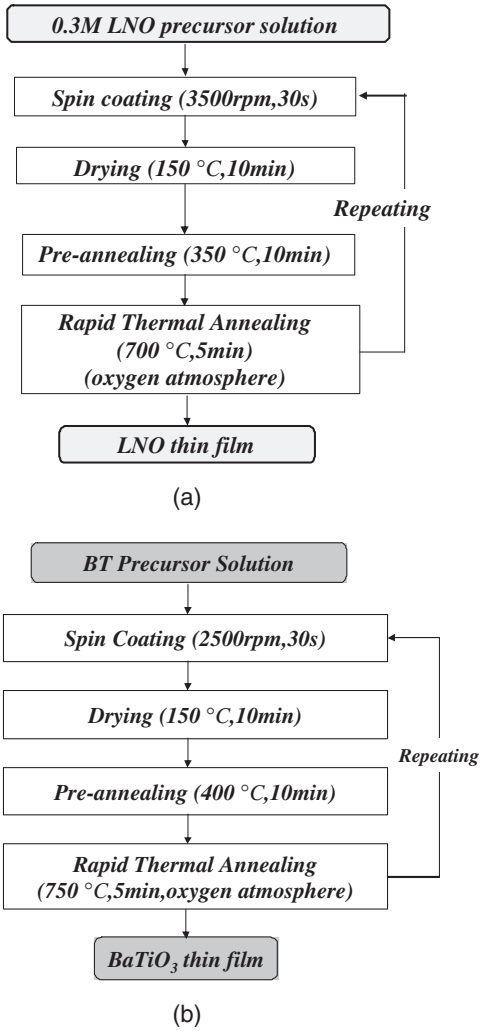

Fig. 2. Film preparation by spin coating for LNO electrode (a) and BT film (b).

99.0%) and refluxing at 125°C for 1 h in a separable flask. CH_3COOH (acetic acid, Kanto Chemical Co. Inc., 99.7%) of 2 times high molar amount compared to the Ti alkoxide was added to the refluxed solution and the solution was kept refluxed for another 1 h at the same temperature. After cooling down the solution to room temp., distilled water of equimolar to the Ti alkoxide was added to the solution and stirred for 3 h at room temperature. The Ba and Ti precursor solutions were then mixed and stirred in the ice bath.

The precursor solutions for the BT films and the LNO electrodes prepared by the processes above were spin coated on the Si (100) substrate (called as Si substrate hereafter) or the $Pt/Ti/SiO_2/Si$ substrate (called as Pt substrate hereafter) as schematically shown in **Fig. 2**(a) and (b). LNO precursor solution was spin coated (3500 rpm, 30 s) on the substrate and dried (150°C, 10 min). The dried film was pre-annealed (350°C, 10 min.) using an electric furnace and annealed (700°C, 5 min.) in oxygen atmosphere by a Rapid Thermal Annealing (RTA). Multi layer stacking (1, 2, 4, 6 layers) was achieved by repeating the whole deposition process (spin coating, drying, pre-annealing, and annealing). The thickness of one LNO layer can be considered about 50 nm from our previous experiments. BT film preparation was similar to the LNO except for spinning speed (2500 rpm), pre-annealing temperature (400°C), and annealing temperature (750°C). The number of stacking layer of the BT film was 15 layers, which resulted in about 250 nm thickness.

Crystal structure of the obtained film was studied by X-ray diffraction (XRD). Lattice parameter and crystallite size of the BT film was calculated from XRD patterns of the (002)/(200) peaks using TOPAS analysis software (Bruker AXS K.K.). Indices to show orientation of the BT film along the (001) and (100) planes were introduced by the following scheme,

$$Orientation\ (hkl) = \frac{I_{(hkl)}}{I_{(100)(001)} + I_{(110)} + I_{(111)}}$$

where the I values indicates peak intensity in the 2θ–θ XRD patterns.

Observation of microstructure of the films was studied by FE-SEM. Elemental distribution of the films was observed by STEM-EDS. Dielectric and ferroelectric properties of the film were measured by an impedance analyzer (HP 4194A, Agilent Technologies Inc.) and a ferroelectric properties analyzer (FCE-1, Toyo Corporation), respectively. For measurement of the electrical properties, Au top electrode was coated by sputtering.

3. Results and discussion

Figure 3 shows XRD patterns of the BT/LNO film on Si (a) and Pt (b) substrate. From the XRD patterns, it can be recognized that BT and LNO were successfully fabricated on both Si and Pt substrates. Both of the BT and LNO were highly oriented along the ⟨100⟩ and ⟨001⟩ direction. Orientation and crystallite sizes of the BT film were calculated as shown in **Table 1**. These values

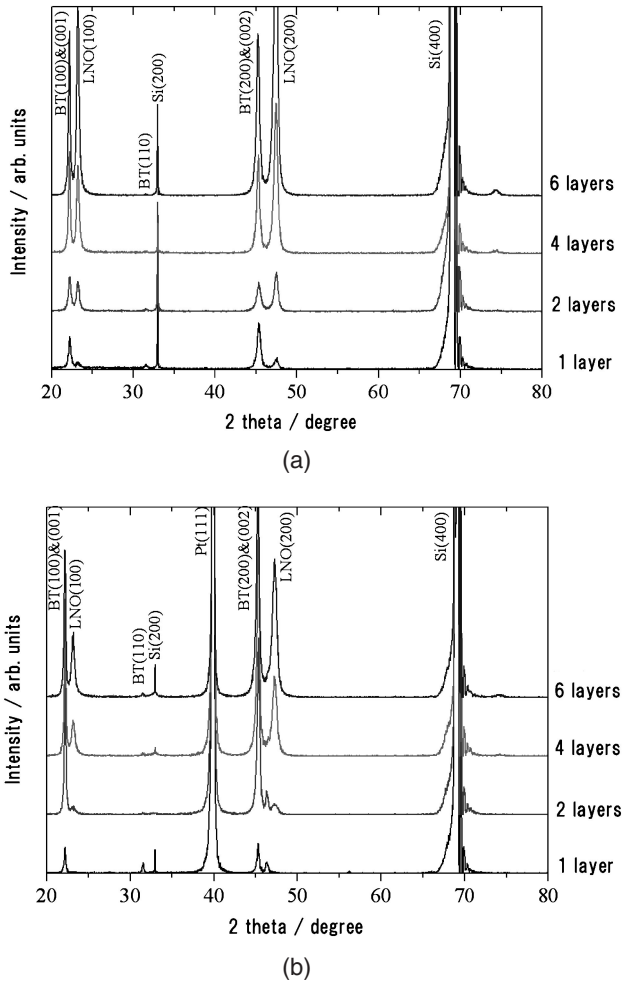

Fig. 3. XRD patterns of the BT/LNO films on Si (a) and Pt (b) substrates. The number of the layer indicates the number of the stacking layers of LNO.

Table 1. Orientation and crystallite size of the BT films

LNO thickness (nm)		Orientation of BT(001)&(100) (%)	Crystallite size (nm)
Si substrate	50 (1 layer)	90	24
	100 (2 layers)	96	22
	200 (4 layers)	99	25
	300 (6 layers)	99	24
$Pt/Ti/SiO_2/Si$ substrate	50 (1 layer)	84	33
	100 (2 layers)	99	39
	200 (4 layers)	99	42
	300 (6 layers)	99	33

Table 2. Lattice parameters of the BT films

LNO thickness/nm		a axis/nm	c axis/nm	c/a
Si substrate	100 (2 layers)	3.9875	3.9961	1.0022
	200 (4 layers)	4.0005	4.0106	1.0025
	300 (6 layers)	4.0026	4.0134	1.0027
$Pt/Ti/SiO_2/Si$ substrate	100 (2 layers)	3.9885	4.0048	1.0041
	200 (4 layers)	3.9919	4.0113	1.0049
	300 (6 layers)	4.0009	4.0192	1.0046

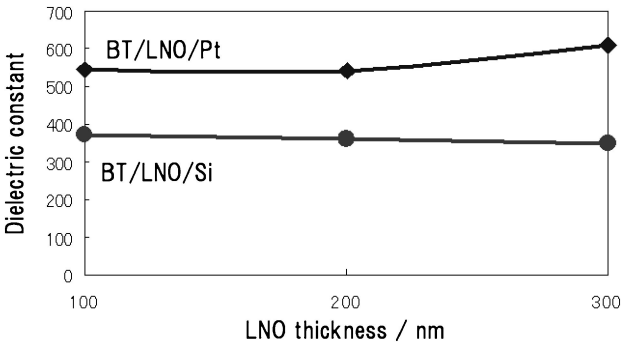

Fig. 4. Dielectric constant of the BT films with various LNO thickness.

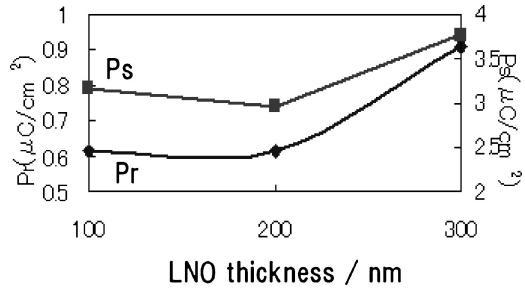

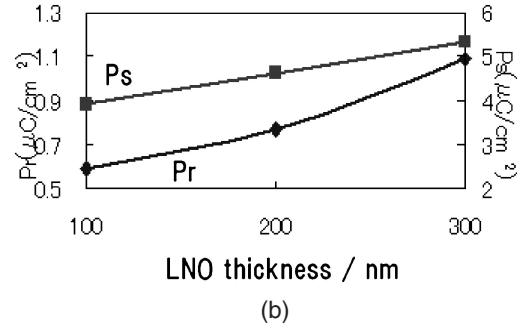

Fig. 5. Ferroelectric properties of BT films with various LNO thicknesses on Si (a) and Pt (b) substrates. Ps and Pr indicate saturation polarization and remnant polarization, respectively.

indicated that on each substrate, the orientation of the BT film increased with increasing the number of LNO layers. The reason of this correlation between the number of LNO layer and orientation of the BT film is considered that the orientation of the LNO bottom electrode; the LNO tends to become uniaxial orientation[35] and the tendency increases with increasing LNO layers, therefore the film on it becomes high orientation. Crystallite sizes were independent of the LNO layer numbers, but increased when the film was prepared on the Pt substrate. Lattice parameter of the BT film was shown in **Table 2**. The lattice parameters, a and c, increased with increasing LNO layer numbers which might be caused by the compressive stress applied from LNO to the film due to the difference of the thermal expansion coefficient between the BT, LNO, and substrate.[35),36)]

Dielectric and ferroelectric properties of the BT film with various LNO layer number were shown in **Fig. 4** and **Fig. 5**(a) and (b), respectively. The dielectric constant increased independent of LNO thicknesses when the film was prepared on the

Pt substrate. This is considered that relatively large crystallite sizes of the BT film on Pt substrate (ave. 24 nm on Si and ave. 37 nm on Pt) resulted in the high dielectric constant. Regarding the ferroelectric values, P_r and P_s, they are not large enough for strict discussions at this moment. However, the tendency that the P_s and P_r totally increased with increasing LNO layer numbers might be caused by the BT lattice expansion along with the vertical direction due to the compressive stress in plane. One may think it is unreasonable that the dielectric constant increased with increasing the LNO layer number because it leads lattice expansion vertical to the plane which usually decreases the dielectric constant. It can be understood by considering the fact that the crystallite sizes of the BT films also increased with increasing LNO layer numbers, which resulted in high dielectric constant. In other words, at least two factors simultaneously act on the BT film by the LNO: generation of compressive stresses in plane and improvement of crystallite size. Further study regarding the electrical properties in detail and lattice deformation observation by the HRTEM is under investigation.

Figure 6 shows cross sectional FE-SEM images of the BT/LNO(2 layers)/Pt sample. Although interfaces between BT, LNO, and Pt is not clear, dense BT and porous LNO structure can be observed. **Figure 7**, STEM-EDS images, supplies further information about the film morphology. The STEM-BF image and the elemental mappings show infiltration of the Ba into the LNO layer, and the Ti and O into the Pt layer.

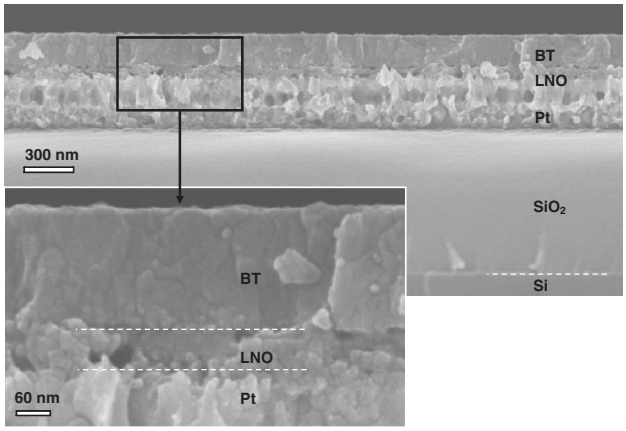

Fig. 6. Cross sectional FE-SEM images of the BT film on LNO(2 layers)/Pt substrate.

From the STEM images, the porous LNO structure seems that it allowed infiltration of the Ba and Ti into the bottom layers which implies reducing the electric properties of the film, but it can also be considered that the porous structure of the LNO induced compressive stresses to the BT film and enhanced the ferroelectric properties similar to the PZT/LNO/Si system as reported by Ohno et al.[35] As described in the electrical properties part, further investigation is required to totally understand the electrical properties and microstructures of the BT film (including an effect of compressive stresses) and it is in progress.

4. Conclusion

BT films and LNO electrodes were fabricated on Si and Pt substrates by the CSD method. Orientation of (100) and (001) of the BT film increased with increasing LNO layer numbers. XRD patterns showed the BT film was subjected to a compressive stress applied by the LNO electrode. Crystallite size of the BT film on the Pt substrate was larger than that on Si substrate. Dielectric constant of the BT film on the Pt substrate was high compared to that on Si substrate, which seemed to be caused by the different crystallite sizes. P_r and P_s of the BT films showed a tendency to increase with increasing LNO layer numbers, which might be caused by a compressive stress applied to the BT film from the LNO electrode. FE-SEM and STEM-EDS observation also implied that the porous LNO structure might apply the compressive stress to the BT film. Further investigation will be required in order to understand interactions among electrical properties, microstructures, and compressive stresses.

References

1) M. Dawber, K. M. Rabe and J. F. Scott, *Rev. Mod. Phys.*, **77**, 1083–1130 (2005).
2) M. W. Cole and R. G. Geyer, *Mech. Mater.*, **36**, 1017–1026 (2004).
3) F. Jin, G. W. Auner, R. Naik, N. W. Schubring, J. V. Mantese, A. B. Catalan and A. L. Micheli, *Appl. Phys. Lett.*, **73**, 2838–2840 (1998).
4) H. Chazono and H. Kishi, *Jpn. J. Appl. Phys., Part 1*, **40**, 5624–5629 (2001).
5) R. Ueyama, K. Koumoto, K. Yubuta and T. Fujii, *J. Ceram. Soc. Japan*, **111**, 282–284 (2003).
6) X. H. Wang, R. Z. Chen, Z. L. Gui and L. T. Li, *Mater. Sci. Eng., B*, **99**, 199–202 (2003).
7) H. Ohsato, N. Ozaki, K. Ohnuma, Y. Mizuno, T. Hagiwara, K. Kakimoto and H. Kishi, *Ferroelectrics*, **302**, 511–516 (2004).
8) S. S. Park, *Integr. Ferroelectr.*, **74**, 95–102 (2005).

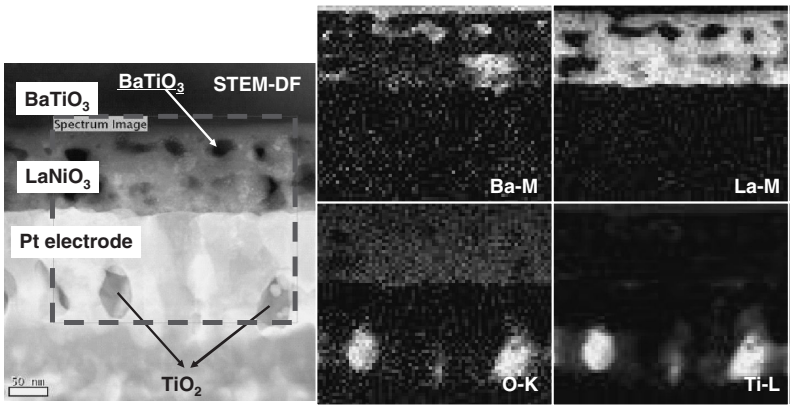

Fig. 7. STEM-DF and EDS mapping (Ba, La, O, and Ti). Mapping area was indicated by the square with dashed lines in the STEM-DF image.

9) H. Kakemoto, T. Harigai, J. Li, S. M. Nam, S. Wada and T. Tsurumi, *Jpn. J. Appl. Phys., Part 1*, 46, 7097–7100 (2007).
10) H. Kishi, Y. Mizuno, T. Hagiwara, H. Orimo and H. Ohsato, *J. Electroceram.*, 21, 22–28 (2008).
11) F. Nakasone, K. Kobayashi, T. Suzuki, Y. Mizuno, H. Chazono and H. Imai, *Jpn. J. Appl. Phys.*, 47, 8518–8524 (2008).
12) G. Yang, Z. X. Yue, Z. L. Gui and L. T. Li, *J. Appl. Phys.*, 104, 074115 (2008).
13) A. V. Polotai, T. H. Jeong, G. Y. Yang, E. C. Dickey, C. A. Randall, P. Pinceloup and A. S. Gurav, *J. Electroceram.*, 23, 6–12 (2009).
14) K. Sugimura and K. Hirao, *J. Ceram. Soc. Japan*, 117, 1039–1043 (2009).
15) T. Wang, X. H. Wang, H. Wen and L. T. Li, *Int. J. Miner., Metall. Mater.*, 16, 345–348 (2009).
16) S. Yamazoe, S. Oda, H. Sakurai, H. Adachi and T. Wada, *J. Ceram. Soc. Japan*, 117, 66–71 (2009).
17) D. Alonso-Sanjose, R. Jimenez, I. Bretos and M. L. Calzada, *J. Am. Ceram. Soc.*, 92, 2218–2225 (2009).
18) Y. P. Guo, D. Akai, K. Sawada and M. Ishida, *Solid State Sci.*, 10, 928–933 (2008).
19) Y. P. Guo, K. Suzuki, K. Nishizawa, T. Miki and K. Kato, *Integr. Ferroelectr.*, 88, 51–57 (2007).
20) O. Y. Jun, R. Ramesh and A. L. Roytburd, *Appl. Surf. Sci.*, 252, 3394–3400 (2006).
21) P. K. Sharma, G. L. Messing and D. K. Agrawal, *Thin Solid Films*, 491, 204–211 (2005).
22) Y. Sakai, T. Futakuchi, T. Iijima and M. Adachi, *Jpn. J. Appl. Phys., Part 1*, 44, 3099–3102 (2005).
23) Y. P. Guo, K. Suzuki, K. Nishizawa, T. Miki and K. Kato, *J. Cryst. Growth*, 284, 190–196 (2005).
24) K. Tanaka, K. Suzuki, D. S. Fu, K. Nishizawa, T. Miki and K. Kato, in "Electroceramics in Japan Vii," Vol. 269, ed. by M. Miyayama, T. Takenaka, M. Takata and K. Shinozaki (2004) pp. 57–60.
25) K. Tanaka, K. Suzuki, D. S. Fu, K. Nishizawa, T. Miki and K. Kato, *Jpn. J. Appl. Phys., Part 1*, 43, 6525–6529 (2004).
26) R. Pantou, C. Dubourdieu, F. Weiss, J. Kreisel, G. Kobernik and W. Haessler, *Mater. Sci. Semicond. Process.*, 5, 237–241 (2002).
27) J. Yu, X. J. Meng, J. L. Sun, Z. M. Huang and J. H. Chu, *J. Appl. Phys.*, 96, 2792–2799 (2004).
28) P. Muralt, T. Maeder, L. Sagalowicz, S. Hiboux, S. Scalese, D. Naumovic, R. G. Agostino, N. Xanthopoulos, H. J. Mathieu, L. Patthey and E. L. Bullock, *J. Appl. Phys.*, 83, 3835–3841 (1998).
29) S. Y. Chen, *Mater. Chem. Phys.*, 45, 159–162 (1996).
30) H. Suzuki, Y. Kondo, S. Kaneko and T. Hayashi, in "Ferroelectric Thin Films Viii," Vol. 596, ed. by R. W. Schwartz et al., Materials Research Society, Warrendale (2000) pp. 241–246.
31) W. Gong, J. F. Li, X. C. Chu, Z. L. Gui and L. T. Li, *Acta Mater.*, 52, 2787–2793 (2004).
32) A. D. Li, C. Z. Ge, P. Lu, D. Wu, S. B. Xiong and N. B. Ming, *Appl. Phys. Lett.*, 70, 1616–1618 (1997).
33) W. Y. Park and C. S. Hwang, *Appl. Phys. Lett.*, 85, 5313–5315 (2004).
34) T. Schneller and R. Waser, *Ferroelectrics*, 267, 293–301 (2002).
35) T. Ohno, B. Malic, H. Fukazawa, N. Wakiya, H. Suzuki, T. Matsuda and M. Kosec, *J. Ceram. Soc. Japan*, 117, 1089–1094 (2009).
36) Y. Sakamaki, H. Fukazawa, N. Wakiya, H. Suzuki, K. Shinozaki, T. Ohno and M. Kosec, *Jpn. J. Appl. Phys., Part 1*, 46, 6925–6928 (2007).